

Experimental study on rheology behaviour geogrids and numerical analysis of reinforced earth structures by visco-elasto-plasticity FEM

Luan, M.T., Xiao, C.Z. & Yang, Q.

State Key Laboratory of Coastal and Offshore Engineering, Dalian University of Technology, Dalian 116024, China.
School of Civil Engineering, Hebei University of Technology, Tianjin 300310, China

Pei, J.J.

Qingdao Etsong Geogrids Co., Ltd., Qingdao 266111, China

Shangguan, Y.L.

Communications Scientific Research Institute of Jinlin Province, Changchun 130022, China

Keywords: geogrids, reinforced earth retaining wall, rheology/creep, visco-elasticity, finite element method

ABSTRACT: Geogrids are widely used to reinforce earth structures as reinforcements. Experimental tests of creep behaviour of geogrids were performed under different combinations of loads and environmental temperatures. Based on the tests results, characteristics of creep curves, load-strain curves and relaxation curves of geogrids are comprehensively compared. By using the fundamental of visco-elasticity, a visco-elastic constitutive model of geogrid is proposed to reproduce its creep behavior and dependence of the model parameters on environmental temperature is examined. Then, for geosynthetics-reinforced earth retaining walls, a two-dimensional FEM-based numerical method is developed. In the study, a visco-elasto-plasticity model is used for backfills while the proposed visco-elastic model is employed for geogrids. Therefore long-term performance of geogrid-reinforced earth retaining walls is analyzed. As an illustrative example, the Denver test wall comprising of cohesive soils is investigated by the proposed method.

1 INTRODUCTION

Geosynthetics, which have been widely applied in geotechnical engineering to reinforced earth structures such as embankments, slopes, and retaining walls, will display creep characteristics. Therefore, creep characteristics of geosynthetics will play an important role in governing long-term performance of reinforced earth structures. Recently, some experimental studies on the creep behavior of geosynthetics have been reported. Creep tests of geotextiles have been carried out by Das (1990) and Leshchinsky and *et al.* (1997) to establish creep model. Based on accelerated creep tests, a comparative experimental study on geosynthetics products such as geogrids was performed by Wang (1994) and Wrigley and *et al.* (1999). These experimental results are instructive for engineering practices. At the same time, in order to well understand performance of reinforced retaining walls and principles of reinforcement, related studies were made on geosynthetics reinforced flexible structures. By using FEM, deformation and bearing capacity behavior were analyzed by Karpurapu and Bathurst (1995) and Rowe and Skinner (1987) respectively for geosynthetics reinforced retaining walls directly founded on rigid foundation and constructed on a clay foundation. However, both viscous effects including rheology of backfills and geosynthetics reinforcements are not taken into consideration in

most of the previous analyses based on FEM. Helwany and Wu (1995) attempted to evaluate long-term performance of reinforced earth structures by using rheologic models. However, these numerical analyses cannot authentically reproduce the main characteristics of reinforced earth walls.

2 EXPERIMENTAL TEST OF GEOGRIDS

The domestic product unidirectional geogrids made of the material of HDPE are selected for the specimen of geogrids. According to the ISO13431 standard, the specimen including at least 3 ribs with the width of less than 0.2 m and length of 1.5 m are included. The engineering properties of the test geogrids are listed in Table 1.

For each selected type of geogrid specimen, three load levels which respectively correspond to 40%, 50% and 60% of ultimate tensile strength of the geogrid and three different temperatures of 20°, 40°

Table 1. Engineering properties of geogrids.

Types of geogrid	Tensile strength R_{ult} ($\text{kN}\cdot\text{m}^{-1}$)	Tensile strength of Wide-Width strip ($\text{kN}\cdot\text{m}^{-1}$)		Loading levels (percentage of R_{ult}) (%)		
		2%	5%			
		EG90R	88.0	23.7	45.2	40
EG65R	64.5	16.1	30.9	40	50	60

and 50° are used in the creep tests. The Test duration is controlled to no shorter than 1000 hours. The test loads are applied with steel weights directly on the specimens as shown Figure 1. Specimens are attached to the loading device using a clamping system composed of a steel bar with bolts and nuts. The tensile pullout force in unit width is defined as $R = (PD_r)/N_r$, where P , D_r , and N_r are respectively average applied load, the numbers of tensile elements in unit width and in the specimen. In this tests, D_r and N_r are 48.94 ribs/m and 3 ribs respectively.

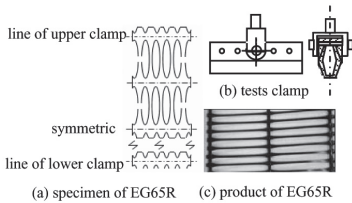


Figure 1. Schematic diagram of creep test.

3 TESTS RESULTS AND ANALYSES

3.1 Creep properties of geogrid

The test results obtained from the above creep experiments under different environmental temperatures for EG65R geogrid are displayed in Figure 2 for three load levels.

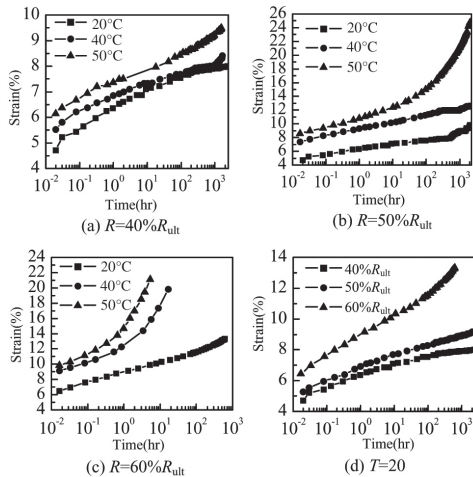


Figure 2. The variation of creep strain of EG65R with time.

It is found that creep curves of all the specimens subjected to the above mentioned three load levels exhibits a tendency of linearly increase with time before the strain of 10%. However, over than 10%, creep strain of specimen increases with time in a more noticeable rate. As illustrated in Figure 2(a), under the same load level of 40% of ultimate tensile strength of geogrid, the strain will attain to 8%

respectively after about 1500, 700 and 40 hours for the environmental temperature of 20, 40, and 50°C respectively. It is implied that the effect of temperature on creep strain appears to be remarkable. It can be observed from Figure 2 that at the same environmental temperature, the time required to attain a specified strain under lower load level, e.g. 40% of ultimate tensile strength, is much longer than that under higher load levels, e.g. 50% and 60% of the ultimate tensile strength. Therefore, the load level will considerably affect creep behavior of geogrid.

3.2 Isochronous curves and stress relaxation curves

Based on the creep tests of EG65R geogrids, both isochrones curves and stress-relaxation curves are given in Figure 3. It can be seen that the isochrones curves seems to display a rather similar tendency for different instants. During initial loading phase, strain varies with time elapsing remarkably and then becomes smoothly with no sharp. At the same time, under the initial loads of 40%, 50% and 60% of ultimate tensile strength, the creep strain rate of EG65R geogrids appears to be very low after a certain period of loading, e.g., 100 hours. It is evident that stress-relaxation curves at the strain of 4%, 5% and 6% are similar.

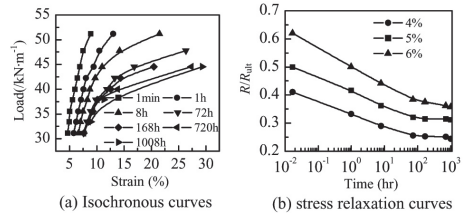


Figure 3. Isochrone and stress relaxation of geogrids EG65R.

3.3 Visco-elastic constitutive model for geogrids

Based on the experimental data, the following empirical nonlinear visco-elastic model with three unknown parameters is proposed for geogrids

$$R = E_0 \varepsilon^b \frac{1}{1 + \left(\frac{t}{t_0}\right)^\beta} \quad (1)$$

Where R and ε denote the force per unit width and strain of geogrids respectively, t is the elapsed time, E_0 , b , t_0 and β are model parameters related to material properties. As proposed by Dechasakulsom (2001), $\beta = 0.1$ is appropriate for polymer such as HDPE. For geogrids EG65R, the model parameters at three specified environmental temperatures of 20, 40 and 50° are given in Table 2.

3.4 Effect of temperature on model parameters

Based on the experimental data, the dependence of the three parameters in the proposed empirical model

Table 2. Model parameters for geogrids EG65R.

Types of geogrids	Temperature (C°)	Model parameters		
		<i>b</i>	<i>t</i> ₀	<i>E</i> ₀
EG65R	20	0.62	395	295
	40	0.48	3.76e6	126
	50	0.43	4.96e7	98

on environmental temperature is shown in Figure 4. The data are fitted by with exponential type. It is obvious that the three parameters are closely associated with temperature. With rise of temperature, the parameters, *b* and *E*₀, decrease with approximately negative exponential functions while the parameter *t*₀ increases with an approximately positive exponential function.

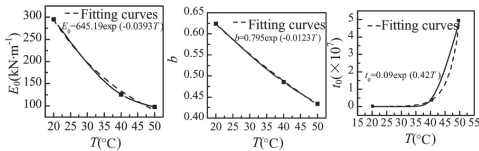


Figure 4. Variation of model parameters with temperature.

4 FEM-BASED NUMERICAL PROCEDURE

In order to consider the rheological property of backfills, the rheological model with five-elements proposed by Nishihara, as shown in Fig. 5, is adopted for soils. At the same time, the empirical nonlinear visco-elasticity model for geogrids established above is employed to consider the creep behaviour of reinforcement in the reinforced earth wall. In addition, the joint element model proposed by Goodman *et al.* is used for the interfaces between reinforcement and backfills, panel and backfills as well as panel and panel in order to rationally consider interaction effects. The construction process of backfills of retaining wall is also simulated by layer-by-layer filling. Nonlinear analyses based on 2-D FEM are numerically implemented by a hybrid algorithm in which the incremental scheme is incorporated with iterations by using the initial-strain procedure. Based on these analyses, a two-dimensional FEM-based numerical method is developed.

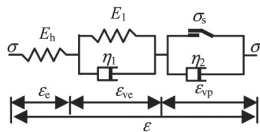


Figure 5. Nishihara's rheological model of soil.

4.1 Model parameters of the Denver test walls

For the Denver test walls, the confined compression tests of cohesive soils are simulated by using the Nishihara's model as shown in Figure 5. Through fitting of simulated results to experimental data, the five parameters of soil are specified in which four deformation parameters are *E*_h = 1.5 MPa, *E*₁ = 4.1

MPa, *η*₁ = 68.9 MPa-d, *η*₂ = 15.8 MPa-d while the yield strength of soils, *σ*_s, will be defined by Drucker-Prager criterion with strength parameters of *c* = 51.5 kPa and *φ* = 15°.

For geotextiles used in the Denver text wall, the parameters in the proposed model can be determined by comparing the simulated creep curves and isochrones curves with the given creep experimental data as shown in Figure 7. The three parameters of *E*₀, *b* and *t*₀ are defined as 17.8, 0.51 and 2.62, respectively.

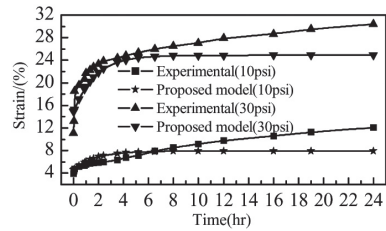


Figure 6. Comparison of variations of strain with time simulated with test results for the Denver wall.

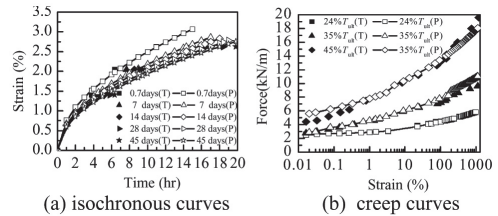


Figure 7. Comparison of test data with simulated results of geotextile for Denver wall (T: Test; P: Proposed).

The panel of the Denver wall made by timbers and plywood are assumed to be isotropic linear elastic material. The elastic modulus and Poisson's ratio are 13.69 MPa and 0.25 respectively.

The nonlinear characteristics of the shear behaviour of the interface between the reinforcement and backfill is considered in the shear stiffness given by the following empirical formulae

$$K_s = k_s \gamma_w \left(\frac{\sigma_n}{p_a} \right)^n \left(1 - \frac{R_f \tau}{\tau_f} \right)^2 \quad (2)$$

For the Denver wall, parameters for the interface elements between reinforcement and soil are determined by direct shear tests as follows: *c* and *φ* are 17.2 kPa and 27°, *k*_s, *n* and *R*_f are 8130, 0.88 and 0.75 respectively. Parameters for contact faces between panel and backfills and between panels are used, *i.e.*, *c* and *φ* are 0.5 kPa and 30° respectively and tangential and normal stiffness coefficients of the interfaces are 2000 kPa and 10,000MPa respectively.

4.2 Analysis of numerical results

For the Denver test wall, the finite element model together with the specified displacement boundary conditions is shown in Figure 8. In numerical analyses,

the surcharge with the intensity of 15 psi is applied step-by-step by 5 increments in addition to 12 increments after accomplishment of construction. The 100 hours of sustained load is divided into 300 increments. In Figure 9 and Figure 10, the computed vertical displacements at the top of the backfill and the lateral movements of the panel are compared with measured data. Although the measured vertical displacements near the wall are significantly less than those farther from the wall, the computed vertical displacements seem to display the same tendency with observed data. Both the computed vertical displacements of the backfill and lateral deformations of the wall are overall reasonable.

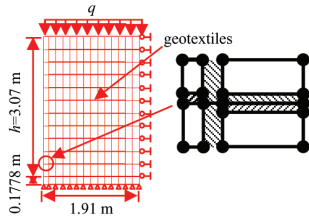


Figure 8. FEM model of the Denver wall.

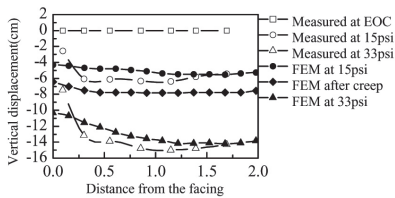


Figure 9. Vertical displacements at the top of backfills.

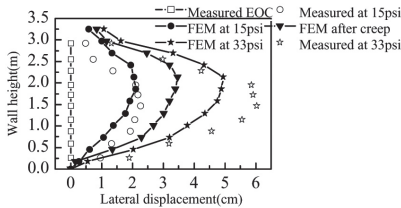


Figure 10. Lateral displacement of panel for the Denver wall.

For the Denver wall, the strains in the reinforcements at three elevations above the base of the wall were measured. At the end of application of the load, the computed strains of the reinforcements at different elevations are compared with the measured results as shown in Figure 11. It is obvious that the measured strains tend to vanish at the end of the geotextiles. The simulation can agree well with the measured data, especially in the neighborhood of the middle of geotextiles.

5 CONCLUDING REMARKS

The experimental results of rheology of geogrids indicate that both loading level and temperature play

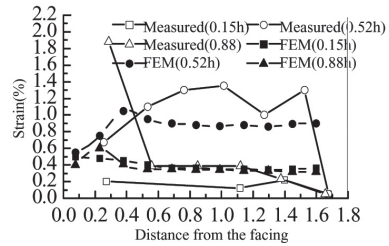


Figure 11. Simulated and measured strain distribution at different elevations under the surcharge of 15 psi.

an important role in controlling rheologic behaviour of the geogrids. An empirical viscoelastic constitutive model with three unknown parameters is proposed to reproduce rheologic characteristics of the geogrid. Effects of temperature on the parameters of the proposed model are examined.

A FEM-based numerical procedure for analysis of long-term performance of reinforced earth structures is presented in this paper. A case study is performed based on the parameters of backfills and geotextiles as well as interfaces specified for the Denver test wall. Through the comparison of the computed results with measured data, the validity of the proposed procedure is verified. The proposed numerical procedure can be employed to evaluate the long-term deformation and bearing capacity behaviour of reinforced earth structures when both creep characteristics of geosynthetics and the rheologic property of backfills are considered.

REFERENCES

- Das M. (1990). "Creep behavior of geotextiles." *Proceedings of the 4th International Conference on Geotextiles*, The Hague, PP. 667-674.
- Dechaskulsom Montri. (2001). "Modeling time-dependent behavior of geogrids and its application to geosynthetically reinforced walls." Dissertation of University of Delaware, USA.
- Helwany M.B. and Wu J.T.H. (1995). "A numerical model for analyzing long-term performance of geosynthetic reinforced soil structures." *Geosynthetic International, Journal of the International Geosynthetics Society*, 2(2), PP. 429-453.
- Karapur R. and Bathurst R.J. (1995). "Behaviour of geosynthetic reinforced soil retaining walls using the finite element method". *Computers and Geotechnics*, 17, PP. 279-299.
- Leshchinsky D., Dechaskulsom M. and Kaliakin VN., et al. 1997. "Creep and stress relaxation of geogrids." *Geosynthetics International*, 4(5), PP. 463-579.
- PRENV 13431. (1998). International Organization for Standardization: Geotextiles and Related Products Determination of Tensile Creep and Creep Rupture Behavior.
- Rowe R.K. and Graeme D. Skinner. (2001). "Numerical analysis of geosynthetic reinforced retaining wall constructed on a layered soil foundation." *Geotextiles and Geomembranes*, 19(6), PP. 387-412.
- Wang Zhao. (1994). "The creep tests of geosynthetics". *Chinese Journal of Geotechnical Engineering*, 16(6), PP. 96-102.
- Wrigley N.E., Austin R.A., Harrison P.E. (1999). "The long-term strengths of geogrid reinforcement." *Geosynthetics '99*, PP. 711-721.